Electrochimica Acta 202 (2016) 310–315

Contents lists available at ScienceDirect

Electrochimica Acta

journal homepage: www.elsevier.com/locate/electacta

Preliminary research on the use of SVET in non-aqueous media

A.C. Bastos*, M.C. Quevedo, M.G.S. Ferreira

DEMaC – Department of Materials and Ceramic Engineering and CICECO – Aveiro Institute of Materials, University of Aveiro, 3810-193 Aveiro, Portugal

ARTICLE INFO

Article history:
Received 29 September 2015
Received in revised form 6 December 2015
Accepted 14 December 2015
Available online 17 December 2015

Keywords:
Ethanol
Corrosion
Organic solvent
SVET
Scanning vibrating electrode technique
Surface coatings

ABSTRACT

An investigation is presented on the use of the scanning vibrating electrode technique (SVET) in non-aqueous media, namely pure ethanol and ethanol saturated with NaCl. The SVET was able to measure the ionic currents flowing in the liquid phase between anodes and cathodes in electrochemical systems such as platinum disk electrodes connected to a battery, a zinc–iron galvanic couple, painted galvanised steel with artificial defects and alumina coated cast aluminium alloy. The results show the applicability of the technique in non-aqueous highly resistive medium.

1. Introduction

The Scanning Vibrating Electrode Technique (SVET) is used in corrosion research since the early 1980s after the work of Hugh Isaacs [1–4]. It has been applied to characterise many corrosion systems of localized nature as, for example, galvanic corrosion [5–8], pitting corrosion [9–12], crevice corrosion [13], stress corrosion cracking [14], microbiologically influenced corrosion [15], inorganic coatings [6,16,17], organic coatings [18–21], corrosion inhibitors [22–24], and conducting polymers [25,26]. Another field where the SVET is used, and in fact where it was developed, is biology and the life sciences, where it is known as vibrating probe and is applied in areas like electrophysiology [27–31], morphogenesis [32–34], cellular differentiation [35], tissue regeneration and would healing [29,36–38].

In all cases, the medium, either corrosion environment or biological fluid, is of aqueous nature but this is not a requisite. Since SVET measures the electrical field in solution associated to the electrical current flowing therein, it should work in any liquid crossed by a current. Notwithstanding, no references can be found with SVET measurements in non-aqueous medium. This paper describes a series of experiments performed in organic medium to analyse the SVET operation in such conditions.

2. Experimental

2.1. Non-aqueous media

The testing media were either pure ethanol (99.99%, Fisher Chemical) with a theoretical conductivity of 1.4×10^{-9} S cm^{-1} [39] or pure ethanol saturated with NaCl (p.a. grade reagent, >99,8%, Sigma–Aldrich) with a conductivity of 2.4×10^{-4} S cm^{-1} (23.5 °C) measured with Inlab 731 conductivity probe connected to SevenMulti Meter from Mettler Toledo. The reported solubility of NaCl in pure ethanol is 0.55 g/Kg$_{solvent}$ [40]. Ethanol was the chosen solvent because it is easily available, relatively safe and has a moderate evaporation rate. It is polar and protic, like water, which seems advisable for first trials.

2.2. Materials and samples

Four different samples were analysed in this work. The first comprised two platinum wires of 1 mm diameter embedded in epoxy resin (EpoKwick, Buehler, USA) and electrically connected to a battery, as shown in Fig. 1a). The second sample was similar to the first except that 1 mm pure iron and 1 mm pure zinc wires (99.99+%, Goodfellow, UK) were used in place of the platinum wires. The surfaces of the embedded metallic wires were abraded to 1200 grit finish with SiC paper, washed in distilled water followed by pure ethanol. A third sample consisted of 1×1 cm^2 piece of coil-coated steel. The steel sheet was 800 μm thick with 7.5 μm layer of electrodeposited zinc and 20 μm thick epoxy paint pigmented with TiO_2. Nine small defects were manually produced with a needle. The sample was glued to an epoxy holder with an

---

* Corresponding author. Tel.: +351 234378146.
E-mail address: acbastos@ua.pt (A.C. Bastos).

http://dx.doi.org/10.1016/j.electacta.2015.12.107

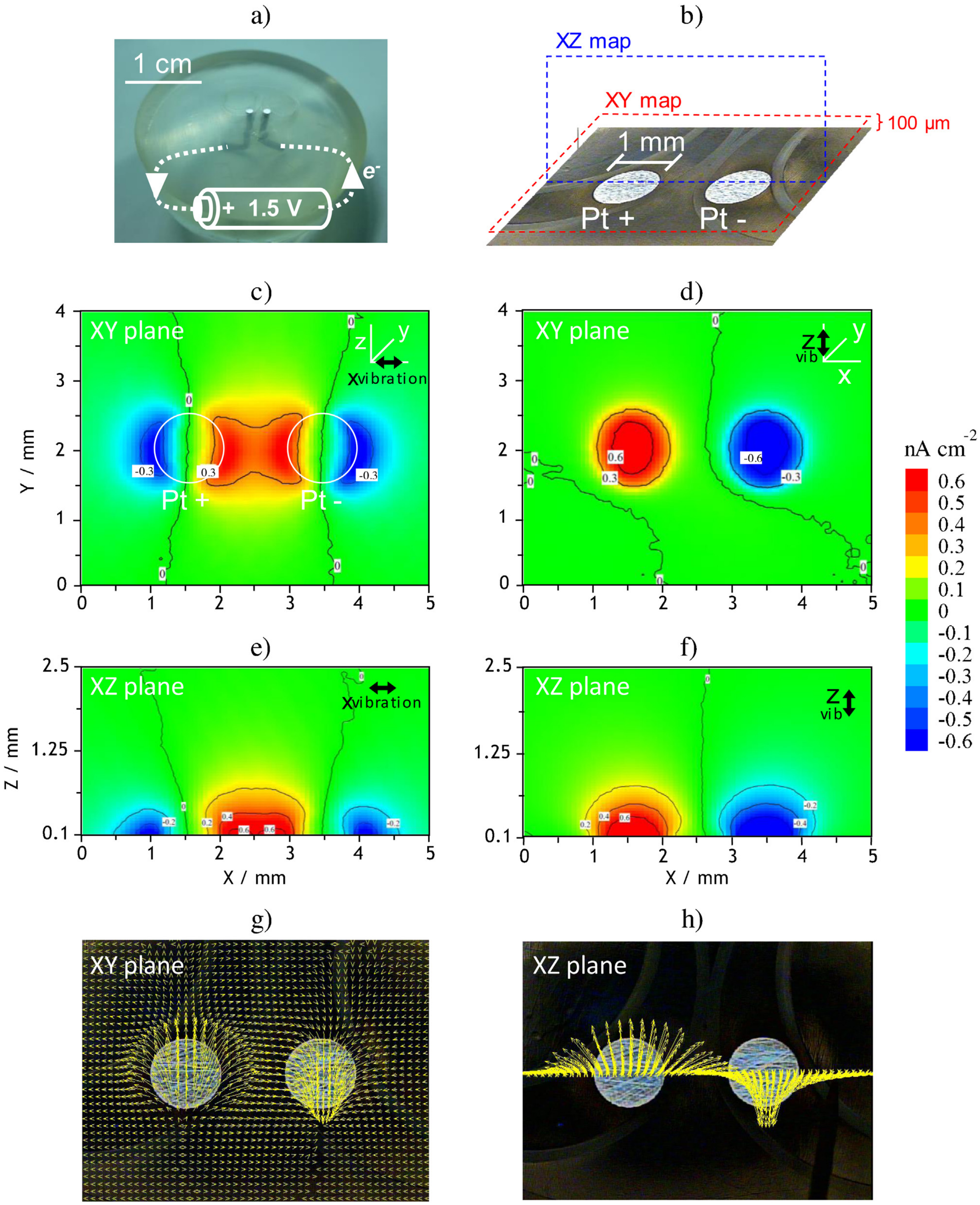

Fig. 1. SVET measurements over Pt electrodes connected to a battery in pure ethanol ($\kappa = 1.4 \times 10^{-9}$ S cm^{-1},[39]); a) test cell consisting of two platinum disks of 1 mm diameter embedded in epoxy resin and connected to 1.5 V battery; b) position of SVET maps measured above the 2 platinum disks in the plane parallel to the surface (XY) and a plane normal to the surface (XZ); c)-f) current density maps measured in the two planes depicting the x and z current density components measured by each SVET vibration; g)-h) 2D vectors of the same current density shown in c)-f).

embedded wire which allowed electrical connection from the back. The edges were protected with epoxy cement and further isolated with varnish (Lacomit, Agar Scientific, UK). The forth sample was a piece of LM24 cast aluminium alloy (AlSi8Cu3Fe) coated with 100 µm thick layer of alumina (Al_2O_3) deposited by plasma spraying. The sample was glued to an epoxy holder with electrical connection and the edges were isolated with a mixture of beeswax and colophony in a proportion 3:1 by weight. Adhesive tape around the epoxy embeds and holders served as solution reservoir.

2.3. SVET measurements

The SVET equipment was manufactured by Applicable Electronics Inc. (USA) and controlled by the ASET 2.00 program developed by Sciencewares (USA). The SVET probe was a polymer insulated Pt-Ir microelectrode with 20 µm diameter platinum black sphere at the tip. The microelectrode vibrated in two directions, one parallel (x axis) and another normal (z axis) to the sample surface, sensing the electric field in the two directions. The x and z frequencies were 115 Hz and 69 Hz, respectively, and the amplitude of both vibrations was 10 µm. After arriving to a point of measurement the probe waited 0.2 s and then averaged for 0.2 s before moving to the next point. The measured potential differences were converted to current densities after a calibration [41]. The calibration is valid for a new solution provided the system is updated with its conductivity. In this work the probe scanned 100 or 200 µm above the surface and maps comprised 20 × 20 points (5 minutes acquisition) up to 60 × 60 points (30 minutes). The acquisition time depends on the map size, number of points, and sampling rules (wait and averaging times in each point).

To perform the measurements with the first sample, the platinum electrodes were connected to the poles of a common 1.5 V battery. SVET measured in two planes above the electrodes – Fig. 1b). In the second sample the zinc and iron electrodes were either left isolated or connected during the SVET measurements. In samples three and four, a current was made to pass between the working electrode (the coated sample electrically connected from the back) and a platinum wire, in a two-electrode arrangement, with Ivium CompactStat potentiostat (The Netherlands).

3. Results

This section presents some examples of possible uses of SVET in non-aqueous media. The first example illustrates the characterisation of a model cell consisting of two platinum disk electrodes in ethanol connected to a battery. The application to corrosion science and technology is highlighted by the analysis of iron and zinc corrosion in ethanol when the two metals are either isolated or galvanically coupled. A third example shows the application of the technique to detect defects and pores in coatings applied on conductive substrates.

3.1. SVET analysis of a model electrochemical cell in ethanol

Fig. 1 shows results of the first experiment designed to check what SVET measures when two platinum disks are immersed in pure ethanol and current is made to pass between them. The electrochemical cell used is represented in Fig. 1a). The objective was to use a very simple set-up for a clear visualisation and understanding of the results. SVET maps were acquired in planes normal and parallel to the Pt disk electrodes as sketched in Fig. 1b). Since SVET vibrates in two directions it is possible to show the x and z current density components in each plane. This is presented in Figs. 1c)-f). Anodic currents are positive (in red) and cathodic currents negative (in blue). The maps with the z component (z vibration) show positive currents above the positive electrode and negative currents above the negative electrode, as expected. The current regions have symmetrical shapes with the current density decreasing in solution with the distance to the source. Maps of the electrical field are similar to those of the current density, just with a different scale, since the two quantities are directly proportional, as described by equation (1),

$$i_{(x,z)} = \kappa E_{(x,z)} = -\kappa \Delta V / \Delta r_{(x,z)} \tag{1}$$

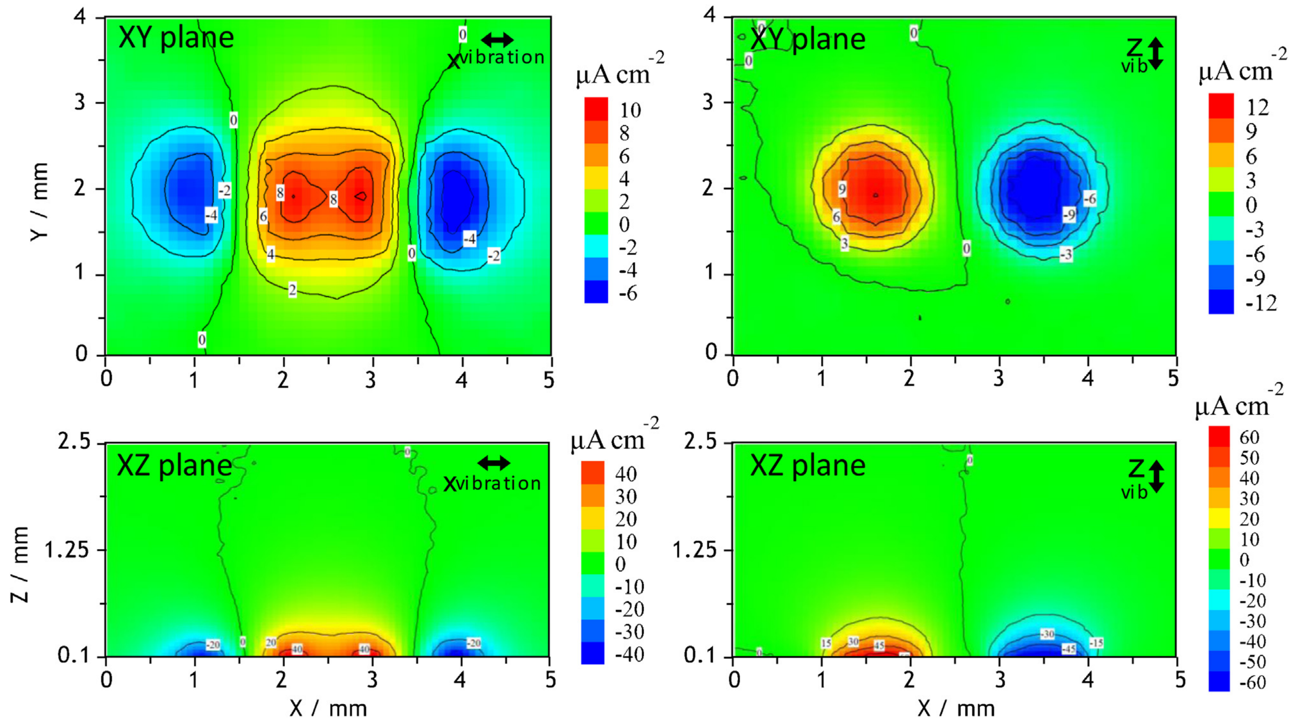

Fig. 2. SVET maps of the x and z current density components in the planes parallel (height = 200 µm) and normal to the surface above Pt electrodes connected to a battery while immersed in ethanol saturated with NaCl (C_{NaCl} = 0.55 g/$Kg_{ethanol}$ [40], κ = 3.03 × 10^{-4} S cm^{-1}).

where *i* is the current density, *E* is the electrical field, κ is the medium conductivity (the proportionality factor between *i* and *E*) and ΔV is the potential difference measured between 2 points distanced by Δr in the direction of the current component of interest (x or z). The shapes of the current regions in the SVET maps also resemble that of a concentration gradient of charged species decreasing with distance from the source.

The current density is a vectorial quantity and knowing this helps understand the maps of the x component (x vibration). The flow of positive charges from left to right or negative charges from right to left corresponds to positive currents while negative currents correspond to the flow of positive charges from right to left and negative charges from left to right. In each electrode, part of the current goes to the right keeping the signal and part goes to the opposite direction, changing signal, as depicted in Figs. 1c) and 1 e). The two current components can be presented together in the form of 2D vectors – Figs. 1g) and 1 h) – giving a better illustration of the direction and magnitude of the current flux. The current density is very small, less than 1 nA cm^{-2}, due to the very low conductivity of the solvent, 1.4×10^{-9} S cm^{-1} [39]. This can be increased by adding charge carriers to solution. Fig. 2 shows results of the same experiment using ethanol saturated with NaCl (3.03×10^{-4} S cm^{-1}, at 23.5 °C). The maps are similar to Figs. 1 c)-f) but with currents about 10^5 times higher. Possible electrochemical reactions are the oxidation of ethanol to acetaldehyde or even to acetic acid [42,43] in the positive electrode and the reduction of dissolved oxygen in the negative electrode. The O_2 concentration in ethanol is 1.94 mM (25 ± 2 °C) [44], higher than the 0.255 mM in water for the same temperature [45]. Reduction of ethanol is not likely to occur and reaction of water absorbed by ethanol from air is not considered because the time of testing was too short for any significant water absorption.

3.2. The first hours of corrosion of Fe and Zn in ethanol measured by SVET

The preceding results confirm that SVET can be used in non-aqueous medium, namely with organic solvents. An obvious application is the study of metallic corrosion in this type of environment. As an example, Fig. 3 presents SVET maps of the corrosion of iron and zinc in ethanol, pure or saturated with NaCl. Fig. 3b) shows the SVET map measured 100 μm above the two metals after 12 hours of immersion in pure ethanol. Very small currents, almost indistinct, were measured in some spots, identified by arrows in the map. When the two electrodes were electrically connected – Fig. 3c) – currents were clearly detected, mainly in the border of the electrodes, positive on zinc and negative on iron. A galvanic coupling was formed and the reactions considered to take place are the oxidation of zinc and oxygen reduction at the iron electrode. The currents measured in pure ethanol were small, even for the Zn-Fe couple, owing to the very low conductivity of the medium. The currents increased substantially in NaCl saturated ethanol. Fig. 3e) reveals that both metals are corroding in ethanol, with anodic and cathodic regions in each one. Coupling the two metals leads to higher currents, cathodic on Fe, and mainly anodic on zinc, yet with some cathodic activity as well.

This shows that zinc and iron corrode in contact with ethanol, particularly if salts are present. The corrosion rate is very low but not zero. Other solvents may be corrosive as well and SVET is able

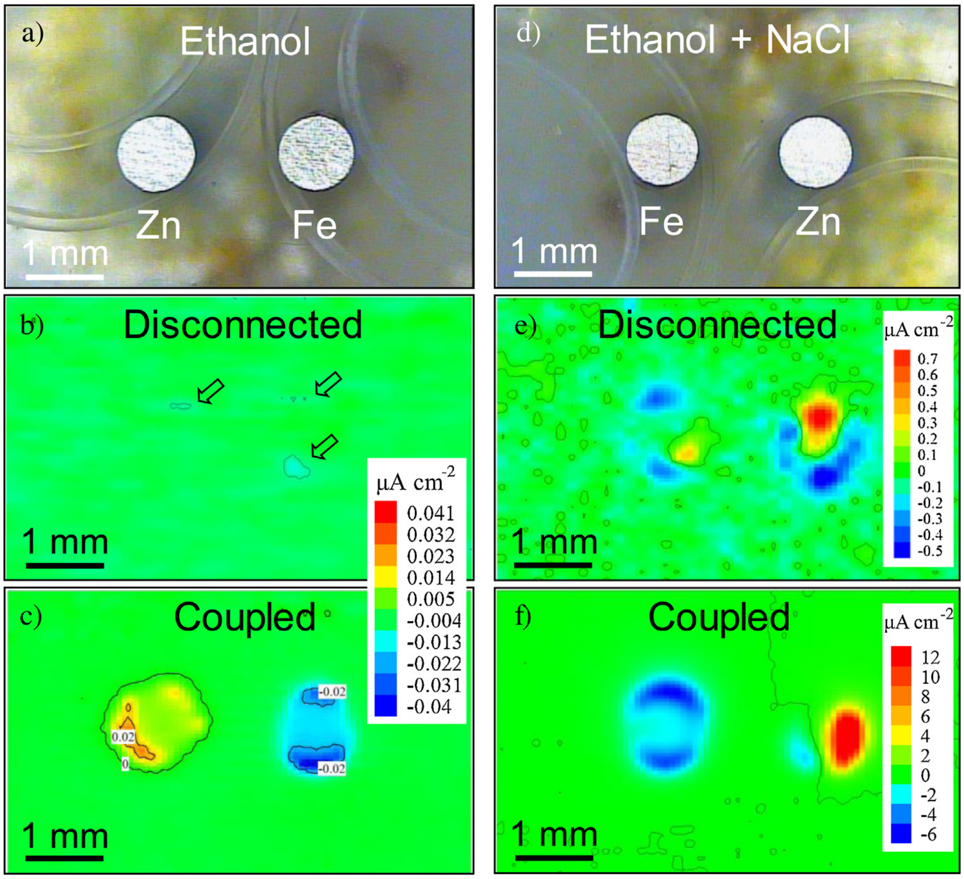

Fig. 3. SVET maps of the corrosion of pure iron and pure zinc after 12 hours of immersion in ethanol without and with NaCl, isolated or galvanically coupled (probe distance to surface = 100 μm).

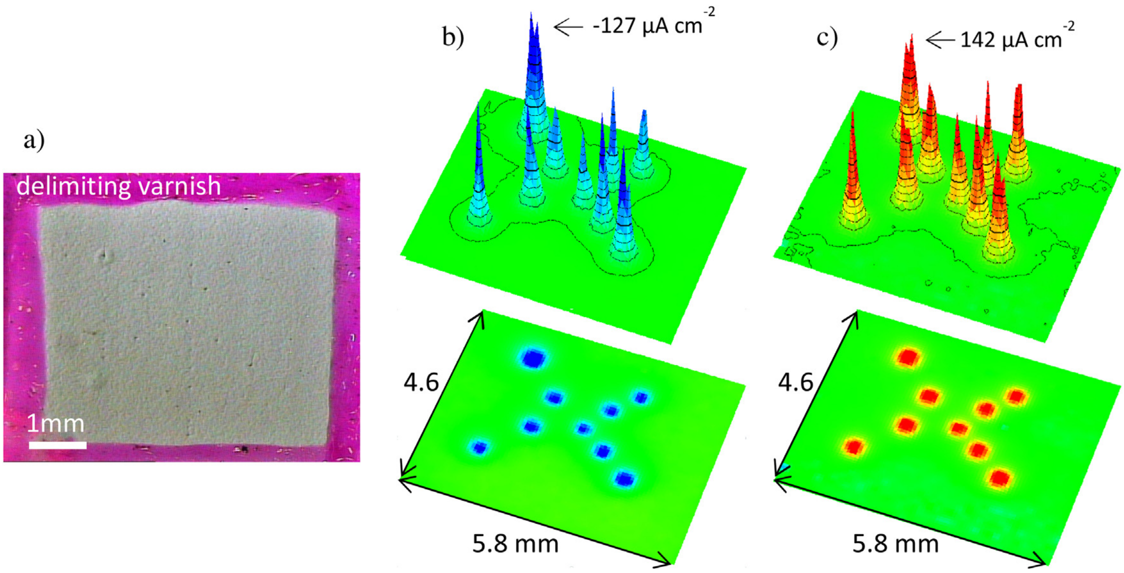

Fig. 4. a) Painted electrogalvanised steel (7.5 µm zinc layer, 20 µm thick TiO_2 pigmented epoxy paint) with 9 artificial defects produced with a needle and SVET maps obtained in a plane 100 µm above the surface during polarization of the sample with −2 µA (b)) or +2 µA (c)).

to analyse the distribution of anodic and cathodic regions on metals of interest and their evolution with time.

3.3. Use of SVET to identify defects and pores in coatings

Corrosion will certainly not take place in many organic solvents, a fact that can be exploited to use SVET for non-destructive testing like the analysis of defects and porosity on coatings applied to metals. There is a great number of techniques to detect and quantify porosity. The intention here is not to present an alternative to them, rather to highlight the possibility of using SVET for the same purpose. Eventually, from time to time, it may be found helpful in very particular circumstances. One example is given in Fig. 4 where nine small defects produced with a needle in a painted electrogalvanised steel sample are easily revealed by SVET after applying a current of 2 µA, either positive or negative. The external polarization is needed for detection since no signals are measured when no current passes in the circuit. Obviously the current should be the minimum possible still giving detectable signals. Another requisite is that the solvent does not interfere with the system under measurement, that is, no reactions with substrate or coating, no swelling and no delamination should occur. In this example blistering was observed in 2 defects, which means that ethanol is not a good medium for tests with this paint. Inorganic coatings are less susceptible to attack by organic solvents. Fig. 5 shows the analysis of the porosity of a Al_2O_3 coat applied by plasma spray on cast aluminium alloy. The SVET map was acquired while a current of 2 µA was made to pass through the coated sample. Since alumina is inert and insulating, the current can only pass if defects and pores are present, revealing them. The porosity is evident in Fig. 5 c). This procedure allows counting the number of pores but the actual size and shape cannot be resolved by this way.

4. Discussion

This work shows that SVET can be used in non-aqueous medium. The mapping of the electrochemical activity on a surface or the measurement at selected points over time can bring new insights of electrochemical systems in these environments. The technique can be employed to study the corrosion in organic or other non-aqueous media. In many cases, corrosion will not occur or will occur at very slow rates. The medium can then be used to perform non-destructive measurements. Exemplary tests were performed to assess the presence of defects or porosity in organic and inorganic coatings applied on conductive substrates. The technique can also be used to characterise the current repartition in solution during electrodeposition, electrosynthesis, or even studies in physical chemistry of non-aqueous electrolytic solutions. Naturally, the judicious choice of solvent and supporting electrolyte is of paramount importance for successful and valuable outcomes of the experiments.

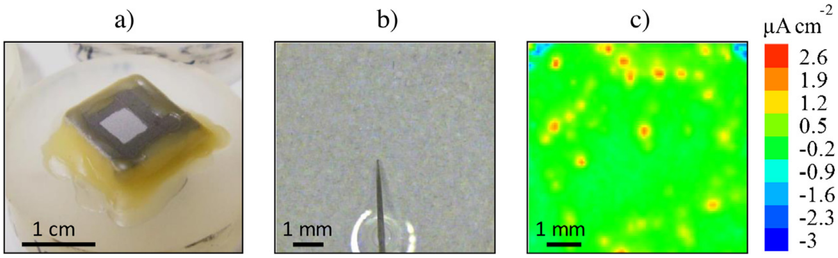

Fig. 5. a) sample of cast aluminium alloy coated with alumina, b) aspect of the coated surface and c) porosity identified as current spots in the SVET map measured when a 2 µA current was passing in the circuit.

5. Conclusions

The use of SVET in non-aqueous media was investigated. This technique was able to measure the currents flowing in the liquid phase between platinum disks connected to a battery or during corrosion of a zinc–iron galvanic couple. It also permitted to locate defects on a paint film and porosity on an alumina layer applied to metal substrates. In these first trials ethanol was used due to its easy availability and non-demanding requirements for the experimental work.

Acknowledgements

M.C. Quevedo thanks CONACYT (Mexico) for the post doc scholarship approach no. 203529 and A.C. Bastos thanks a post-doc grant with the reference BPD/UI50/2739/2013. Funds from Fundação para a Ciência e a Tecnologia (Portugal) project PTDC/CTM-MAT/1515/2012 are also acknowledged.

References

[1] Y. Ishikawa, H.S. Isaacs, Electrochemical behavior of pits developed on aluminum in a dilute chloride solution, Boshoku Gijutsu 33 (1984) 147–152.
[2] H.S. Isaacs, Y. Ishikawa, Paper 55—Applications of the vibrating probe to localized current measurements, Proceedings of NACE Corrosion/85, March, Boston, Massachusetts, USA, 1985.
[3] H.S. Isaacs, Applications of current measurement over corroding metallic surfaces, in: R. Nuccitelli (Ed.), Ionic Currents in Development, A.R. Liss Inc., New York, 1986, pp. 37–44.
[4] H.S. Isaacs, Y. Ishikawa, Application of the vibrating probe to localized current measurements, in: R. Baboian (Ed.), Electrochemical Techniques for Corrosion Engineering, National Association of Corrosion Engineers, Houston, Texas, USA, 1986, pp. 17–23.
[5] H.S. Isaacs, The measurement of the galvanic corrosion of soldered copper using the scanning vibrating electrode technique, Corros. Sci. 28 (1988) 547–558.
[6] K. Ogle, V. Baudu, L. Garrigues, X. Philippe, Localized electrochemical methods applied to cut edge corrosion, J. Electrochem. Soc. 147 (2000) 3654–3660.
[7] D. Battocchi, J. He, G.P. Bierwagen, D.E. Tallman, Emulation and study of the corrosion behaviour of Al alloy 2024-T3 using a wire beam electrode (WBE) in conjunction with scanning vibrating electrode technique (SVET), Corros. Sci. 47 (2005) 1165–1176.
[8] A.M. Simões, A.C. Bastos, M.G. Ferreira, Y. González-García, S. González, R.M. Souto, Use of SVET and SECM to study the galvanic corrosion of an iron - zinc cell, Corros. Sci. 49 (2007) 726–739.
[9] X.-C. Jiang, T. Yoshimura, Y. Ishikawa, T. Shinoharo, S. Tsujikawa, Investigation of alpha prime precipitation in aged duplex stainless steel, J. Electrochem. Soc. 139 (1992) 1001–1007.
[10] A.J. Aldykiewicz Jr., H.S. Isaacs, Dissolution characteristics of duplex stainless steels in acidic environments, Corros. Sci. 40 (1998) 1627–1646.
[11] B. Vuillemin, X. Philippe, R. Oltra, V. Vignal, L. Coudreuse, L.C. Dufour, E. Finot, SVET, AFM and AES study of pitting corrosion initiated on MnS inclusions by microinjection, Corros. Sci. 45 (2003) 1143–1159.
[12] G. Williams, A.J. Coleman, H.N. McMurray, Inhibition of aluminium alloy AA2024-T3 pitting corrosion by copper complexing compounds, Electrochim. Acta 55 (2010) 5947–5958.
[13] H.S. Isaacs, S.-M. Huang, V. Jovancicevic, Location of corrosion on iron and carbon steel surfaces with crevices, J. Electrochem. Soc. 143 (1996) L178–L180.
[14] H.S. Isaacs, Initiation of stress corrosion cracking of sensitized type 304 stainless steel in dilute thiosulfate solution, J. Electrochem. Soc. 135 (1988) 2180–2183.
[15] M.J. Franklin, D.C. White, H.S. Isaacs, Pitting corrosion by bacteria on carbon steel determined by the scanning vibrating electrode technique, Corros. Sci. 32 (1996) 945–952.
[16] H.S. Isaacs, The use of the scanning vibrating electrode technique for detecting defects in ion vapor-deposited aluminum on steel, Corrosion 43 (1987) 594–596.
[17] A.C. Bastos, M.G. Ferreira, A.M. Simões, Effects of mechanical forming on the corrosion of electrogalvanised steel, Corros. Sci. 69 (2013) 87–96.
[18] H.S. Isaacs, A.J. Aldykiewicz Jr., D. Thierry, T.C. Simpson, Measurements of corrosion at defects in painted zinc and zinc alloy coated steels using current density mapping, Corrosion 52 (1996) 163–168.
[19] J. He, V.J. Gelling, D.E. Tallman, G.P. Bierwagen, A scanning vibrating electrode study of chromated-epoxy primer on steel and aluminum, J. Electrochem. Soc. 147 (2000) 3661–3666.
[20] A.C. Bastos, M.L. Zheludkevich, I. Klüppel, G. Grundmeier, M.G.S. Ferreira, Modification of zinc powder to improve the corrosion resistance of weldable primers, Prog Org. Coat. 69 (2010) 184–192.
[21] A.C. Bastos, O.V. Karavai, M.L. Zheludkevich, K.A. Yasakau, M.G.S. Ferreira, Localised measurements of pH and dissolved oxygen as complements to SVET in the investigation of corrosion at defects in coated aluminum alloy, Electroanalysis 22 (2010) 2009–2016.
[22] A.C. Bastos, M.G. Ferreira, A.M. Simões, Corrosion inhibition by chromate and phosphate extracts for iron substrates studied by EIS and SVET, Corros. Sci. 48 (2006) 1500–1512.
[23] A.C. Bastos, M.L. Zheludkevich, M.G.S. Ferreira, A SVET investigation on the modification of zinc dust reactivity, Prog. Org. Coat. 63 (2008) 282–290.
[24] S. Kallip, A.C. Bastos, K.A. Yasakau, M.L. Zheludkevich, M.G.S. Ferreira, Synergistic corrosion inhibition on galvanically coupled metallic materials, Electrochem. Comm. 20 (2012) 101–104.
[25] J. He, V.J. Gelling, D.E. Tallman, G.P. Bierwagen, G.G. Wallace, Conducting polymers and corrosion III. a scanning vibrating electrode study of poly(3-octyl pyrrole) on steel and aluminumucting polymers and corrosion III. a scanning vibrating electrode study of poly(3-octyl pyrrole) on steel and aluminum, J. Electrochem. Soc. 147 (2000) 3667–3672.
[26] J. He, D.E. Tallman, G.P. Bierwagen, Conjugated polymers for corrosion control: scanning vibrating electrode studies of polypyrrole-aluminum alloy interactions, J. Electrochem. Soc. 151 (2004) B644–B651.
[27] L.F. Jaffe, R. Nucitelli, An ultrasensitive vibrating probe for measuring steady extracellular currents, J. Cell Biol. 63 (1974) 614–628.
[28] A. Dorn, M.H. Weisenseel, Advances in vibrating probe techniques, Protoplasma 113 (1982) 89–96.
[29] B. Reid, R. Nuccitelli, M. Zhao, Non-invasive measurement of bioelectric currents with a vibrating probe, Nature Protocols 3 (2007) 661–669.
[30] W. Nagel, P. Somieski, A.M. Shipley, Mitochondria-rich cells and voltage-activated chloride current in toad skin epithelium: analysis with the scanning vibrating electrode technique, J. Memb. Biol. 161 (1998) 131–140.
[31] J.H. Lee, T. Chiba, D.C. Marcus, P2X$_2$ receptor mediates stimulation of parasensory cation absorption by cochlear outer sulcus cells and vestibular transitional cells, J. Neurosci. 21 (2001) 9168–9174.
[32] R. Nucitelli, Ionic currents in morphogenesis, Experientia 44 (1988) 657–666.
[33] K.B. Hotary, K.R. Robinson, Evidence of a role for endogenous electrical fields in chick embryo development, Development 114 (1992) 985–996.
[34] M. Anderson, E. Bowdan, J.G. Kunkel, Comparison of defolliculated oocytes and intact follicles of the cockroach using the vibrating probe to record steady currents, Dev. Biol. 162 (1994) 111–122.
[35] M.J. Saunders, Correlation of electrical current influx with nuclear position and division in *Funaria Caulonema* tip cells, Protoplasma 132 (1986) 32–37.
[36] A. Rubinacci, A. de Ponti, A. Shipley, M. Samaja, E. Karplus, L.F. Jaffe, Bicarbonate dependence of ion current in damaged bone, Calcif. Tissue Int. 58 (1996) 423–428.
[37] M. Levin, Bioelectric mechanisms in regeneration: Unique aspects and future perspectives, Seminars Cell Dev. Biol. 20 (2009) 543–556.
[38] M. Zhao, Electric fields in wound healing - An overriding signal that directs cell migration, Seminars Cell Dev. Biol. 20 (2009) 674–682.
[39] I.M. Smallwood, Handbook of organic solvent properties, Elsevier, 1996.
[40] S.P. Pinho, E.A. Macedo, Representation of salt solubility in mixed solvents: A comparison of thermodynamic models, Fluid Phase Equilibria 116 (1996) 209–216.
[41] Scanning Vibrating Electrode Technique (SVET) Manual, Applicable Electronics Inc, Forestdale, MA, USA, (2006).
[42] S.C.S. Lai, M.T.M. Koper, Electro-oxidation of ethanol and acetaldehyde on platinum single-crystal electrodes, Faraday Discuss 140 (2008) 399–416.
[43] C.H. Mamann, A. Hamnett, W. Vielstich, Electrochemistry, 2nd Ed, Wiley-VCH, 2007 p. 364.
[44] C. Franco, J. Olmsted III, Photochemical determination of the solubility of oxygen in various media, Talanta 37 (1990) 905–909.
[45] M.L. Hitchman, Measurement of Dissolved Oxygen, Vol. 49 in A series of monographs on analytical chemistry and its applications, Wiley and Sons, NY, 1978.